**RAA 2017** Vol. **17** No. **4**, 38 (14pp) doi: 10.1088/1674–4527/17/4/38

*http://www.raa-journal.org* *http://iopscience.iop.org/raa*

***R**esearch in*
***A**stronomy and*
***A**strophysics*

# H$\alpha$ profile variations in the spectrum of the supergiant HD14134

Yanosh Mahmud Maharramov and Gunel Osman Jahangirova

Shamakhy Astrophysical Observatory, Azerbaijan National Academy of Sciences, Yu. Mammadaliyev settlement, Shamakhy district, Azerbaijan; *y_meherremov@rambler.ru*

Received 2016 August 3; accepted 2017 January 17

**Abstract** Variations of the H$\alpha$ line in the spectra of the star HD14134 are investigated using observations carried out in 2013–2014 and in 2016 with the 2-m telescope at Shamakhy Astrophysical Observatory. In the spectra of this star, the absorption and emission components of H$\alpha$ are found to disappear and an inverse P Cyg profile of H$\alpha$ is seen on some observational epochs. Our observations showed that when the H$\alpha$ line disappeared or an inversion of the P-Cyg-type profile is observed in the spectra, the H$\beta$ line is redshifted. When these events appeared, no synchronous variabilities were observed in the spectral parameters of other spectral lines formed in deeper atmospheric layers. In addition, the structures of H$\alpha$, CII (6578.05 Å, 6582.88 Å), SiII (6347.1 Å, 6371.36 Å) and H$\beta$ lines are variable on a timescale of hours, but we did not detect significant variations in the other photospheric lines, as well as in the HeI (5875.72 Å) line. It is suggested that observational evidence for the non-stationary atmosphere of HD14134 can be associated in part with non-spherical stellar wind.

**Key words:** star: HD14134 — supergiant — wind — outflow

## 1 INTRODUCTION

The supergiant star HD14134 is classified as a star with a P Cygni (P Cyg) profile associated with the H$\alpha$ line. The stellar parameters found by Barlow & Cohen (1977), Wilson & Dopita (1985), Tarafdar (1988), Kudritzki et al. (1999), Morel et al. (2004), Crowther et al. (2006) and Galazutdinov et al. (2015) are presented in Table 1.

Morel et al. (2004) presented the results of a long-term monitoring campaign of the H$\alpha$ line in a sample of bright OB supergiants, including HD14134. Notably, the changes result from the combined effect of a varying amount of incipient wind emission and an intrinsically variable underlying photospheric profile, with the relative contribution of these two phenomena varying from one star to another. As a consequence of the large amplitude of the $H_\alpha$ variations observed, a precise determination of the stellar atmospheric parameters will not be generally possible from profile fitting of the Balmer lines in snapshot spectra. The low detection rate may have several explanations, including observational limitations or a loss of coherency in the patterns of variability. The authors note that HD14134 is of particular interest, as it is one of the very few early-type stars clearly exhibiting the same pattern of variability in photometric and spectroscopic modes.

Photometric studies of the star HD14134 identified periodicities of 12.823 and 1.625 d (Morel et al. 2004; Lefèvre et al. 2009).

Kudritzki et al. (1999) found that the wind momentum–luminosity relationship (WLR) varies as a function of spectral type. Wind momenta are strongest for O-supergiants, then decrease from early B (B0 and B1) to mid B (B1.5 to B3) spectral types (including HD14134) and become stronger again for A-supergiants. The slope of the WLR appears to be steeper for A- and mid B-supergiants than for O-supergiants. It can be noted that the spectral type dependence is interpreted as an effect of ionization changing the effective number and the line strength distribution function of spectral lines absorbing photon momentum around the stellar flux maximum. In addition, the Balmer lines of supergiants are analyzed by means of non-local thermodynamic equilibrium unified model atmospheres to deter-

**Table 1** Summary of Previous Works on the Supergiant HD14134

| Parameters | Reference | | | | | | | |
|---|---|---|---|---|---|---|---|---|
| | Barlow & Cohen (1977) | Wilson & Dopita (1985) | Tarafdar (1988) | Kudritzki et al. (1999) | Morel et al. (2004) | Crowther et al. (2006) | Lefèvre et al. (2009) | Galazutdinov et al. (2015) |
| Sp. type | B3Ia | | | B3Ia | B3Ia | B3Ia | | |
| $V$ (mag) | 6.55 | | | 6.57 | 6.55 | 6.55 | | |
| $M_{\rm v}$ (mag) | –7.0 | | | –7.13 | | –7.1 | | |
| $B-V$ (mag) | 0.47 | | | 0.48 | | 0.45 | | 0.45 |
| $E(B-V)$ (mag) | | | | 0.69 | | | | |
| Assoc. | | | | Per OB1 | | | | |
| $P_{\rm phot}$ (d) | | | | | 12.823 | | 1.625 | |
| $\log g$ | | | | 2.20 | | 2.05 | | |
| $T_{\rm eff}$ (K) | | 14500 | | 18000 | 16300 | 16000 | | |
| $\log L_*/L_\odot$ | | 5.14 | 5.14 | 5.48 | 5.24 | 5.28 | | |
| $M_*/M_\odot$ | | | 35 | | 24 | | | |
| $R_*/R_\odot$ | | 58.9 | 59 | 56.2 | 52 | 56.7 | | |
| $M$ ($10^{-6}\ M_\odot$ yr$^{-1}$) | 0.71 | | | 0.15 | 1.45 | | | |
| $v_\infty$ (km s$^{-1}$) | 580 | | | 465 | 465 | 465 | | |
| $v \sin i$ (km s$^{-1}$) | | | | | 66 | 66 | | |
| $V_{\rm esc}$ (km s$^{-1}$) | | 363 | | | | | | |
| $V_{\rm rad}$ (km s$^{-1}$) | | | | | | | | –57 |
| $\xi$ (km s$^{-1}$) | | | | 20 | | 15 | | |
| $V_{\rm rot}$ (km s$^{-1}$) | | | | 60 | | | | 158 |
| $d$ (kpc) | 2.12 | | | | | | | 2.21 |

Notes: Spectral class, apparent magnitude ($V$), absolute magnitude ($M_{\rm v}$), photometric quantity ($B-V$, $E(B-V)$), association, photometric period ($P_{\rm phot.}$), acceleration of gravity at the surface ($\log g$), effective temperature ($T_{\rm eff}$), luminosity ($\log L_*/L_\odot$), mass ($M_*/M_\odot$), radius ($R_*/R_\odot$), mass-loss ($M$), terminal velocity ($v_\infty$), escape velocity from the star and RV of the star ($V_{\rm esc}$ and $V_{\rm rad}$), turbulent velocity ($\xi$), rotation speed ($V_{\rm rot}$) and distance ($d$).

mine the properties of their stellar winds, in particular their wind momenta. Note that we assume the parameters found by Kudritzki et al. (1999) are more reliable, because they used the new unified model code developed by Santolaya-Rey et al. (1997).

In addition, the radial velocities (RVs) in different spectral lines of the supergiant HD14134 are presented in Table 2. A study of medium-dispersion spectra of very bright early-type stars has indicated the presence, to a varying degree, of expansion in the outer layers of their envelopes (Hutchings 1970, 1976). They noted that the Balmer progression and the shifted strong HeI and MgII lines indicate a low-density expanding envelope. There is no definite velocity gradient in the lower layers of the star.

Kontizas & Kontizas (1981) revealed that the star HD14134 exhibits Balmer RV progression with differences in Hβ-H8 varying from 7 to 27 km s$^{-1}$.

We see that there has been little investigation concerning the spectral and photometric observations of HD14134. Most researchers have mainly determined physical parameters of the supergiant star HD14134. Note that due to the variable stellar wind and mass-loss rate, variations in the intensity, RVs and P Cyg profiles of lines of hydrogen, helium and highly-ionized ions are observed in the spectra of hot supergiants. From this point of view, a study of the Hα line is of special interest.

Generally, researchers noted that the profile of the Hα line in the spectra of HD14134 indicates fast variable structure, but the sequence of observations was irregular and inadequate to trace in detail changes in spectra. Therefore they noted that more and systematic observations are needed to investigate this supergiant.

In the present paper, which is a sort of continuation of the above studies, we analyze variations in the Hα line. We also investigate variabilities in the Hβ, HeI 5875.72 Å, CII (6578.05 Å, 6582.88 Å), SiII (6347.1 Å, 6371.36 Å) and others lines which form in deeper effective layers of the star's atmosphere.

**Table 2** RVs of the Different Spectral Lines

| RVs | Reference | | |
|---|---|---|---|
| $V_r$ | Hutchings 1970 | Hutchings 1976 | Kontizas & Kontizas 1981 |
| (km s$^{-1}$) | | | |
| $(H_\alpha)_{min.abs.}$ | –147 | | |
| $(H_\alpha)_{max.em.}$ | +43 | | |
| $H_\beta$ | –72 | –49 | –36.7 |
| | | | –38.5 |
| $H_\gamma$ | –63 | –40 | –40.2 |
| | | | –55.6 |
| $H_\delta$ | –54 | | –52.6 |
| | | | –45.6 |
| $H_\varepsilon$ | –50 | | –45.6 |
| | | | –42.6 |
| $(H)_{limit}$ | | –29 | |
| HeI 5015 | –55 | | |
| HeI 4471 | –53 | | |
| HeI 4026 | –48 | | |
| $(HeI)_{mean}$ | –46.5 | –23 | –44.3±4.9 |
| | | | –43.5±2.7 |
| $(OII)_{mean}$ | –50.8 | –28 | |
| $(NII)_{mean}$ | –48 | –23 | |
| MgII 4481 | | –32 | |
| $(MgII)_{mean}$ | –55 | | |
| $(CII)_{mean}$ | –44 | –20 | |
| $(SII)_{mean}$ | –48 | | |
| $(SiII)_{mean}$ | | –25 | |
| $(SiIII)_{mean}$ | –49 | –26 | |

Our main aim is to study the observed peculiarities of these lines in the spectra. We believe that our results will be of interest for further studies of these remarkable stars.

## 2 OBSERVATIONS AND PROCESSING

Spectral observations of the supergiant HD14134 in 2013–2014 and 2016 were carried out using a CCD detector in the Echelle spectrometer mounted at the Cassegrain focus of the 2-m telescope housed at Shamakhy Astrophysical Observatory (Mikailov et al. 2005). The spectral resolution was $R = 15\,000$ and the spectral range was $\lambda\lambda$ 4700–6700 Å.

One to two spectra of the target stars were obtained on each night. The signal-to-noise ratio was S/N =150–200. The average exposure was 1200–1500 s, depending on weather conditions.

The Echelle spectra were processed with the standard technique using the DECH20 and DECH20t software packages (Galazutdinov 1992). The reduction of the spectra, which included continuum placement, construction of dispersion curves (from the spectra of a hollow-cathode Th+Ar lamp or RV standard stars), and spectrophotometric and position measurements was performed using these packages.

In addition to observations of the target star, in order to check the stability of the instrument we also obtained numerous spectra of standard stars, the day background and comparison spectra. Here the day background is a daily sky solar spectrum. Thus, we recorded the spectrum of a thorium-argon lamp for wavelength calibration. The stability of the wavelength scale was verified by measuring the wavelength centroids of OI and $H_2O$ sky lines. The long-term accuracy achieved for wavelength calibration is of the order of 1 km s$^{-1}$ as derived from the spread of measured RVs of telluric lines in the spectra.

The measurement error for the equivalent widths (W) does not exceed 5%, and error of the RV ($V_r$) is of the order of $\pm 2$ km s$^{-1}$. Here, ($V_r$) are velocities of the absorption minima or emission maxima in the selected

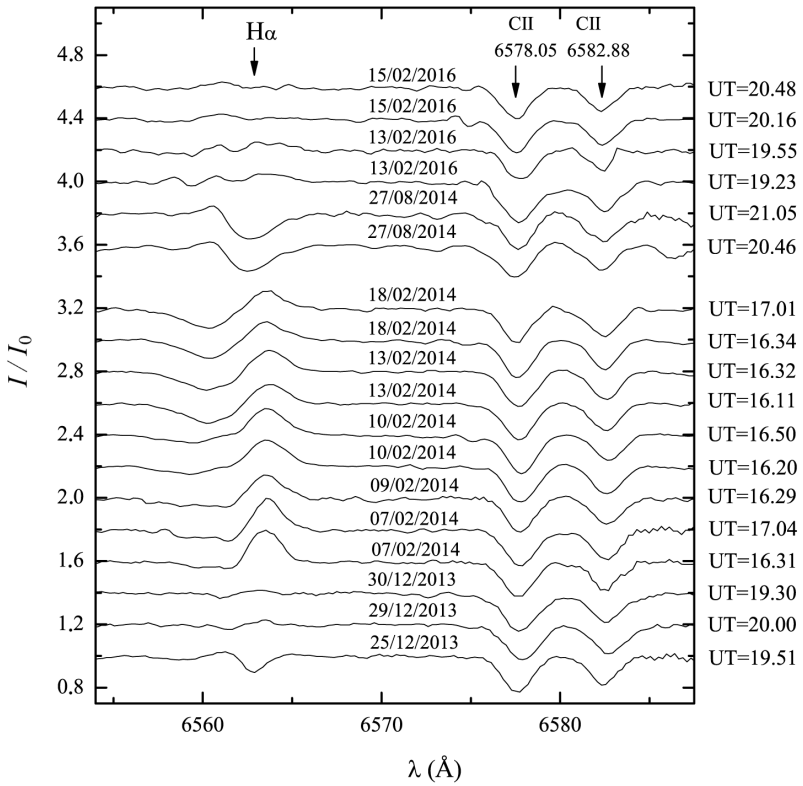


**Fig. 1** Hα and CII (λ6578.05 Å, λ6582.88 Å) profiles in the individual spectra of HD14134 observed in 2013–2014 and 2016.

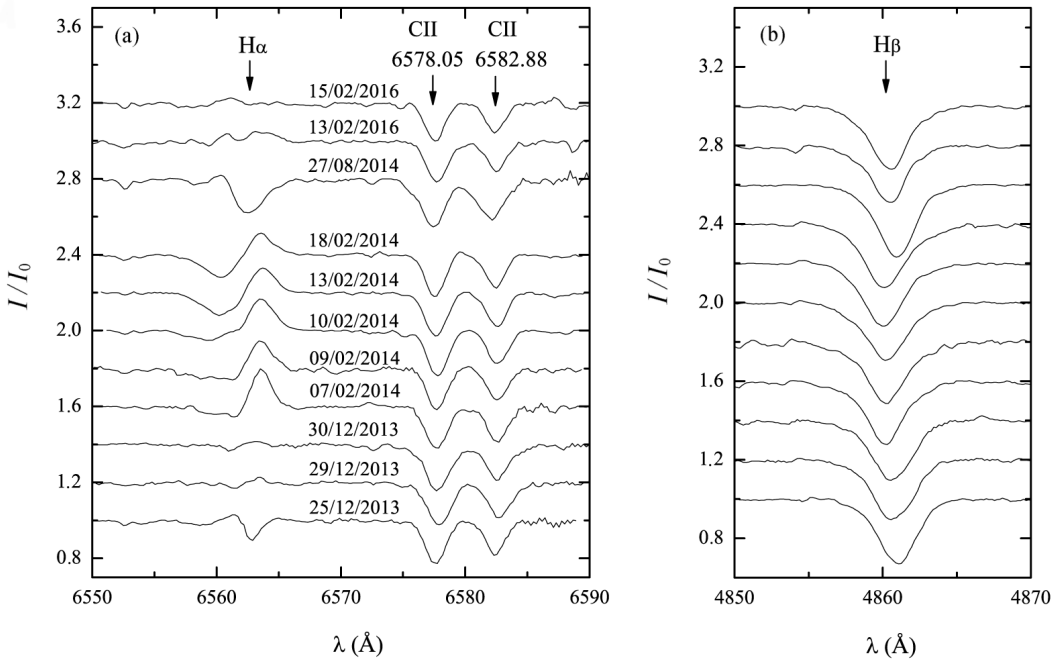


**Fig. 2** Averaged profiles of the Hα, CII (λ6578.05 Å, λ6582.88 Å) and H$\beta$ lines in the spectra of HD14134 observed in 2013, 2014 and 2016.

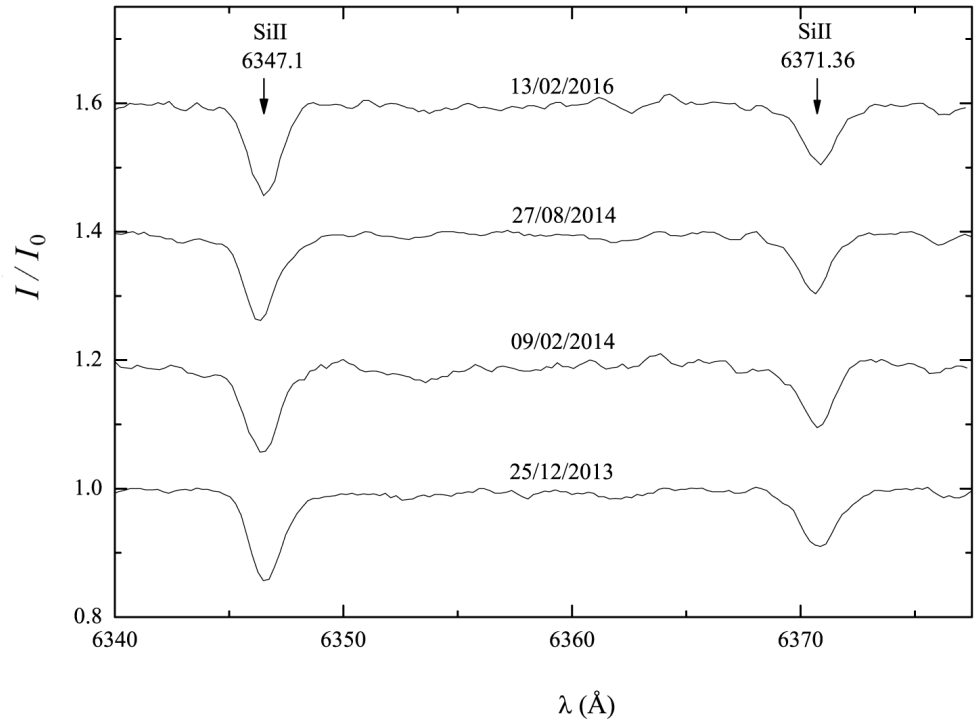


**Fig. 3** Averaged profiles of the SiII ($\lambda$6347.1 Å, $\lambda$6371.36 Å) lines in the spectra of star HD14134.

lines. Note that appropriate heliocentric corrections were included during data processing.

Our observations show that the most pronounced variabilities in the spectra of HD14134 are noticeable in the intensity and profiles of the H$\alpha$ line. The following shapes of the H$\alpha$ profile were observed:

(a) normal P Cyg profile, (b) inverse P Cyg profile, (c) pure absorption profile, (d) pure emission profile, and (e) the emission wings on both sides of the central absorption.

Figures 1 and 2 show the spectra of HD14134 in the wavelength ranges covering the H$\alpha$ and H$\beta$ regions observed in 2013–2014 and in 2016. In Figure 2 the spectra of 2013–12–25, 2013–12–29, 2013–12–30 and 2014–12–09 show individual profiles, but the rest of them are two averaged cases taken during single nights.

The processing of the H$\alpha$ line in the spectrum of HD14134 immediately revealed dramatic changes in profile of this line that occurred with time. On 2013 December 25 and on 2014 August 27, the H$\alpha$ profile in the spectrum of the star HD14134 had the shape of an inverse P Cyg profile. As can be seen in Table 4 and Figure 2(b), at these times a large shift in the H$\beta$ line toward the red was observed simultaneously.

More interesting spectra were obtained on 2013 December 29–30 and on 2016 February 15 (Figs. 1 and 2). The H$\alpha$ line alone is absent from these spectra, and no spectral features are observed at this wavelength (6562.816 Å), except for weak atmospheric lines and noise. At the same time, two strong carbon lines (CII $\lambda$ 6578.05 Å, $\lambda$ 6582.88 Å), as well as several weak stellar and atmospheric lines ($\lambda$ 6542.31 Å, $\lambda$ 6543.91 Å, $\lambda$ 6552.63 Å, etc.) are observed in the spectral order where H$\alpha$ is located, in the region $\lambda\lambda$6400–6600 Å. In these same spectra, all the other lines typical for hot supergiants such as HD14134, apart from H$\alpha$, are observed, including H$\beta$.

In addition, the formation of a very weak emission component associated with the H$\alpha$ line is observed in the spectrum on 2016 February 13 (Fig. 1 and Fig. 2(a)). We suggest this time the emission component became stronger and completely swamped the absorption component. Therefore, no absorption component was observed in the H$\alpha$ profile at this epoch.

In order to investigate the short term variability in the H$\alpha$ profile, all individual spectra obtained on 2013 December 29–30, and on 2016 February 13 and 15 were processed separately. These data are presented in

**Table 3** Measurement of the parameters of the Hα line. Here, the empty rows correspond to observational epochs where Hα is too faint or disappears.

| Date | JD2450000.00+ | $V_r$ abs [km s$^{-1}$] | $V_r$ em [km s$^{-1}$] | $W$ abs [Å] | $W$ em [Å] | $R$ abs | $r$ em | $\Delta\lambda_{1/2}$ abs [Å] | $\Delta\lambda_{1/2}$ em [Å] |
|---|---|---|---|---|---|---|---|---|---|
| 2013–12–25 | 6652.33 | –13 | –87 | 0.14 | 0.03 | 0.10 | 1.02 | 1.3 | 1.0 |
| 2013–12–29 | 6656.33 | – | – | – | – | – | 1.00 | – | – |
| 2013–12–30 | 6657.31 | – | – | – | – | – | 1.00 | – | – |
| | | –91 | | | | | | | |
| 2014–02–07 | 6696.21 | –88 | 11 | 0.14 | 0.35 | 0.05 | 1.20 | 3.4 | 1.7 |
| | | –210 | | | | | | | |
| 2014–02–09 | 6698.19 | –95 | 7 | 0.24 | 0.28 | 0.06 | 1.14 | 4.2 | 1.9 |
| 2014–02–10 | 6699.20 | –179 | 10 | 0.15 | 0.39 | 0.05 | 1.17 | 3.3 | 2.2 |
| 2014–02–13 | 6702.19 | –142 | 17 | 0.36 | 0.28 | 0.12 | 1.13 | 3.1 | 2.1 |
| 2014–02–18 | 6707.21 | –134 | 13 | 0.35 | 0.23 | 0.12 | 1.11 | 2.7 | 1.8 |
| 2014–08–27 | 6897.38 | –31 | –128 | 0.56 | 0.02 | 0.19 | 1.02 | 2.7 | 0.9 |
| 2016–02–13 | 7432.33 | – | – | – | – | – | – | – | – |
| 2016–02–15 | 7434.37 | – | – | – | – | – | 1.00 | – | – |

**Table 4** Measurements of the Parameters of the Hβ Line

| Date | JD2450000.00+ | $V_r$ abs [km s$^{-1}$] | $W$ abs [Å] | $R$ abs | $\Delta\lambda_{1/2}$ abs [Å] |
|---|---|---|---|---|---|
| 2013–12–25 | 6652.33 | –30 | 1.11 | 0.33 | 3.0 |
| 2013–12–29 | 6656.33 | –71 | 1.09 | 0.30 | 3.4 |
| 2013–12–30 | 6657.31 | –74 | 1.10 | 0.30 | 3.3 |
| 2014–02–07 | 6696.21 | –89 | 1.14 | 0.32 | 2.9 |
| 2014–02–09 | 6698.19 | –88 | 1.19 | 0.31 | 3.0 |
| 2014–02–10 | 6699.20 | –90 | 1.11 | 0.29 | 3.3 |
| 2014–02–13 | 6702.19 | –97 | 1.16 | 0.32 | 3.2 |
| 2014–02–18 | 6707.21 | –97 | 1.26 | 0.32 | 3.3 |
| 2014–02–27 | 6897.38 | –40 | 1.27 | 0.37 | 3.0 |
| 2016–02–13 | 7432.33 | –72 | 0.96 | 0.29 | 2.7 |
| 2016–02–15 | 7434.37 | –68 | 1.12 | 0.32 | 2.9 |

Figure 1. It clearly shows that line profile variability is evident already on timescales as short as half an hour, probably due to the presence of pulsations.

Unfortunately, weather conditions before and after 2013 December 29–30 and 2016 February 15 did not make it possible to obtain spectra of the star HD14134, which could shed light on the moments when the transition that is part of this interesting process occurred.

Our measurements show that the RVs and spectral parameters ($W$- the equivalent width, $R$- the depth, $r$- the residual intensity, $\Delta\lambda_{1/2}$- the half-width) of the absorption and emission components of the Hα line, as well as the parameters of lines of other elements, vary with time. However, the largest variations are displayed by the absorption and emission components of the Hα line, which indicate changes of the physical condition in the atmosphere and in the expanding stellar envelope. On 2014 February 07, 09–10 the absorption components of the Hα line are observed in the broader shapes and cases that have weak components (Figs. 1 and 2). Table 3 shows that at those times the depths and equivalent widths of the absorption components of the Hα line relatively decrease, and the emission components relatively increase.

To investigate the reason for variability in the Hα profile, other lines (Hβ, lines of CII, SiII, HeI and others) were analyzed in the spectra. We measured the spectral parameters and RVs of these lines. It is clear that significant changes happened in the RV and spectral parameters

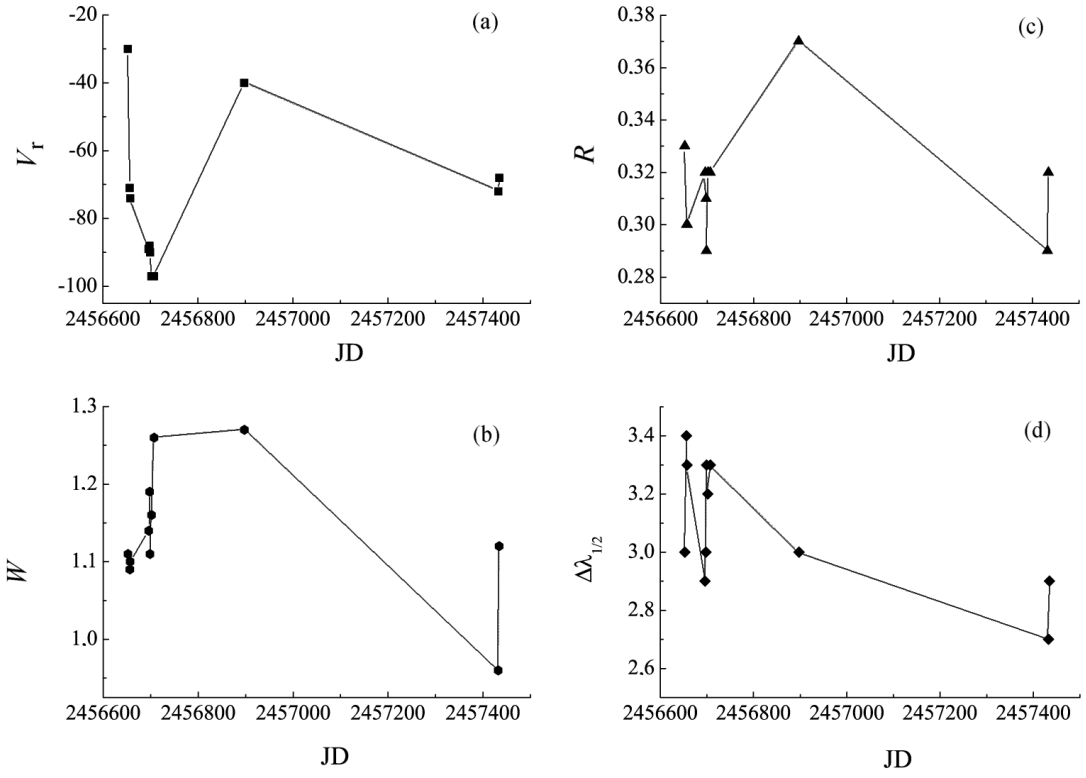


**Fig. 4** Variation with time of the RVs, equivalent widths, depths and half-widths in the H$\beta$ line.

in the H$\alpha$ and H$\beta$ lines. As can be seen from Figure 2(a) and Table 3, sometimes the absorption component of the H$\alpha$ line is observed shifted toward the red side with a speed of –13 km s$^{-1}$, and sometimes this absorption profile had a second component, while the H$\alpha$ line retains a normal P Cyg profile.

Tables 3 and 4 show that the RV of the absorption and emission components of the H$\alpha$ line vary from –179 to –13 km s$^{-1}$, and –128 – 17 km s$^{-1}$ respectively, and the H$\beta$ line varies within –97 to –30 km s$^{-1}$. We have determined that the equivalent width, half-width and depth (in emission the residual intensities) of the absorption component of the H$\alpha$ line vary within 0.14–0.56 Å, 1.3–4.2 Å and 0.05–0.19, the emission component varies within 0.02–0.39 Å, 0.9–2.2 Å and 1.00–1.20, and the H$\beta$ lines vary within 0.96–1.27 Å, 2.7–3.4 Å and 0.29–0.37, respectively. The results are given in Tables 3 and 4.

Figures 1 and 3 show that CII and SiII line profiles vary significantly with time. The RVs of the these lines vary from –46 to –25 km s$^{-1}$ and from $-50$ to $-36$ km s$^{-1}$, respectively.

The investigation of the HeI $\lambda$5875.72 Å line showed that the RV of the line varies from –53 to –35 km s$^{-1}$, and but its profile does not change.

In addition, some of the results of measurements in the spectra of HD14134 are presented on a timescale in Figures 4 and 5. It has been revealed that the variability of RVs, equivalent widths, depths and half-widths of H$\beta$ line, as well as HeI$\lambda$5875.72 Å, averaged CII ($\lambda$6578.05 Å, $\lambda$6582.88 Å) and SiII ($\lambda$6347.1 Å, $\lambda$6371.36 Å) lines indicate repeating features. These cases show that there are variability correlations in the RVs and spectral parameters of the selected lines.

Hence, investigations above showed that this object is spectroscopically variable, in particular, RVs change in different ways with time. Therefore, we also investigated other numerous spectral lines in the considered spectra. We estimated the RVs of the strong and basically weak absorption lines formed in deeper layers of the atmosphere. All measurements are presented in Table 5.

We averaged the values of velocities of all photospheric absorption lines and determined the RV of the star in our observations, $V_r' = -42.2$ km s$^{-1}$. This

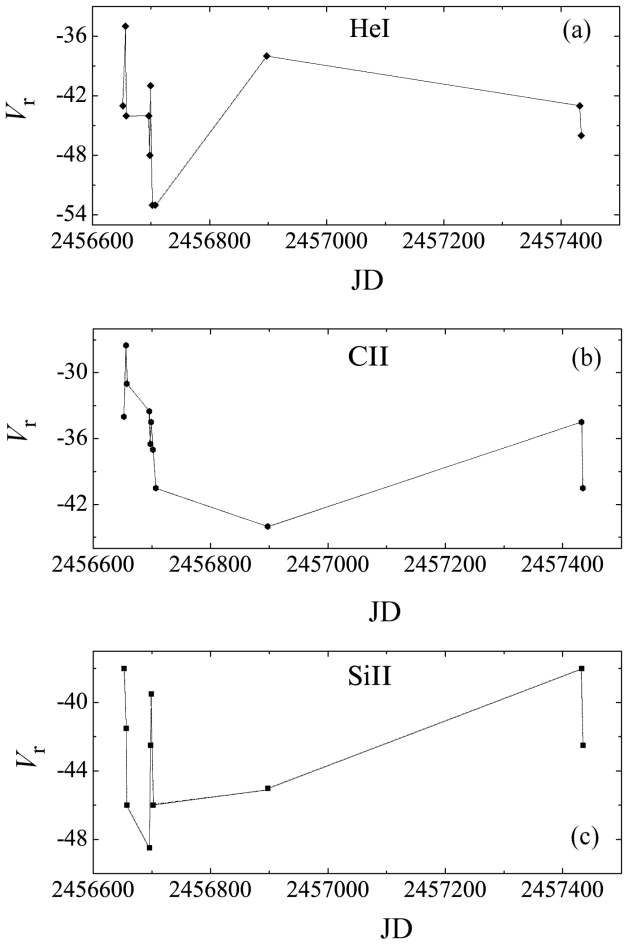


**Fig. 5** Variation with time of the RVs in HeI λ 5875.72 Å and averaged CII (λ6578.05 Å, λ6582.88 Å) and SiII (λ6347.1 Å, λ6371.36 Å) lines in the spectra of HD14134 observed in 2013, 2014 and 2016.

value is close to the velocity of the mass center of the star ($V_{\rm r} = -43.4$ km s$^{-1}$) which is presented in the Gontcharov (2006).

On the other hand, we constructed dependencies of RVs on residual intensities $V_{\rm r}(r)$ for these lines (Fig. 6). If the dependence of $V_{\rm r}$ on $r$ exists, it can be considered as a "kinematic slice" of the atmosphere. It shows that from $r = 0.75$ to $r \to 1$, these changes approach a horizontal straight line with a sharp break. Such form of a curve $V_{\rm r}(r)$ is characteristic of the majority of B-supergiants (Chentsov et al. 2003).

In addition, Table 1 shows that the values of star radius found by different authors are close to each other. Therefore we averaged them and got $R_* = 56.6\ R_\odot$. We found from the references that Kudritzki et al. (1999) and Galazutdinov et al. (2015) determined the rotation velocity of the star (60 km s$^{-1}$ and 158 km s$^{-1}$). However, we assume that the rotation velocity of the star ($V_{\rm rot} = 60$ km s$^{-1}$) found by Kudritzki et al. (1999) is more reliable and we estimated the rotation period of the star.

$$\begin{aligned} P_{\rm rot} &= 2\pi \times R_*/V_{\rm rot} \\ &= 2 \times 3.14 \times 56.6\ R_\odot/60 \times 10^3 \\ &= 6.28 \times 56.6 \times 7 \times 10^8/60 \times 10^3 \approx 48\ ({\rm d}). \end{aligned}$$

We computed phases for this period and gave approximate phase dependence of the variables, but no correlation was found (Fig. 7).

## 3 SPECTRAL ANALYSIS AND DISCUSSION

As has been shown, the shape of the Hα line changed substantially during observations. It displayed an inverse P Cyg-type profile with weak emission on the violet wing (2013 December 25), the Hα profile almost completely

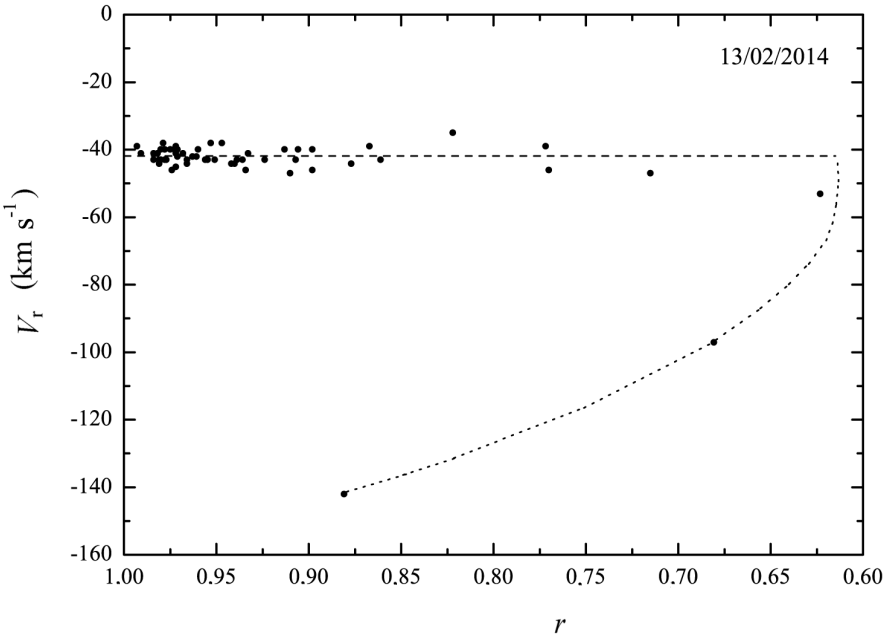


**Fig. 6** Relationship between the RVs and central residual intensities of the absorption lines and absorption components of P Cyg-type profiles in the spectra of HD 14134. Filled circles represent separate lines or components. The dashed line is the averaged velocity. Balmer lines of hydrogen (H$\alpha$ and H$\beta$) are connected with dots.

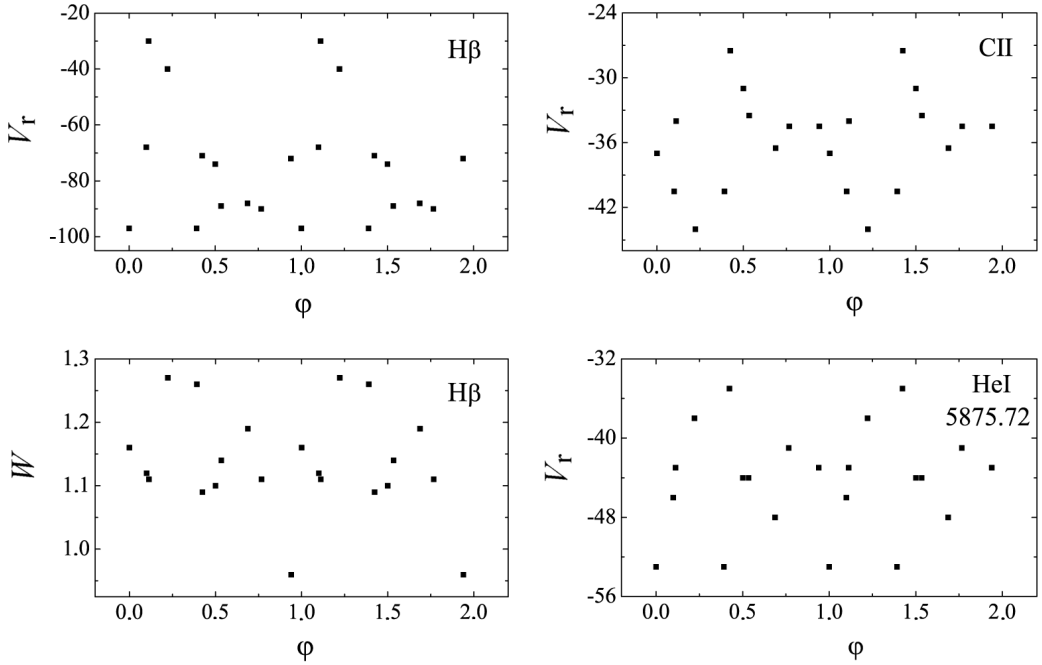


**Fig. 7** Variation with phase ($P_{\rm rot.} = 48$ d) of the RVs, equivalent width in the H$\beta$, averaged CII ($\lambda$6578.05 Å, $\lambda$6582.88 Å) and HeI$\lambda$5875.72 Å. Zero phase is $T_0 = 2456702.19$.

**Table 5** Identification of lines, residual intensities ($r$) and heliocentric RVs ($V_r$) in the spectra of HD14134.

| Lines | λ [Å] | $r$ | $V_r$ [km s$^{-1}$] | Lines | λ [Å] | $r$ | $V_r$ [km s$^{-1}$] |
|---|---|---|---|---|---|---|---|
| CII | 6582.88 | 0.822 | –35 | NII | 5495.67 | 0.979 | –38 |
| CII | 6578.05 | 0.772 | –39 | SII | 5473.62 | 0.960 | –40 |
| Hα | 6562.82 | 0.881 | –142 | SII | 5453.83 | 0.906 | –40 |
| NeI | 6506.53 | 0.966 | –43 | SII | 5432.82 | 0.942 | –44 |
| NII | 6482.05 | 0.953 | –38 | SII | 5428.67 | 0.968 | –41 |
| NeI | 6402.25 | 0.936 | –43 | SII | 5345.72 | 0.982 | –41 |
| NeI | 6382.99 | 0.981 | –44 | SII | 5320.73 | 0.966 | –44 |
| SiII | 6371.36 | 0.898 | –46 | FeII | 5316.65 | 0.993 | –39 |
| SiII | 6347.10 | 0.861 | –43 | FeIII | 5193.89 | 0.980 | –40 |
| NeI | 6163.59 | 0.981 | –43 | FeII | 5169.03 | 0.951 | –43 |
| NeI | 6143.06 | 0.971 | –42 | OII | 5160.02 | 0.991 | –41 |
| NeI | 6074.34 | 0.984 | –43 | FeIII | 5156.12 | 0.947 | –38 |
| HeI | 5875.72 | 0.623 | –53 | CII | 5145.16 | 0.977 | –43 |
| FeIII | 5833.93 | 0.972 | –41 | CII | 5133.12 | 0.978 | –43 |
| NII | 5747.30 | 0.984 | –41 | HeI | 5047.74 | 0.877 | –44 |
| SiIII | 5739.73 | 0.910 | –47 | NII | 5045.10 | 0.939 | –43 |
| AlIII | 5722.73 | 0.934 | –46 | SII | 5027.22 | 0.974 | –46 |
| NII | 5710.77 | 0.956 | –43 | FeII | 5018.44 | 0.971 | –40 |
| AlIII | 5696.60 | 0.898 | –40 | HeI | 5015.68 | 0.770 | –46 |
| NII | 5686.21 | 0.955 | –43 | NII | 5007.33 | 0.973 | –40 |
| NII | 5679.56 | 0.867 | –39 | NII | 5005.15 | 0.933 | –41 |
| NII | 5676.02 | 0.940 | –44 | NII | 5001.40 | 0.907 | –43 |
| NII | 5666.63 | 0.924 | –43 | SII | 4994.36 | 0.975 | –40 |
| SII | 5659.99 | 0.972 | –45 | SII | 4991.97 | 0.980 | –43 |
| SII | 5647.03 | 0.963 | –42 | OII | 4941.12 | 0.978 | –40 |
| SII | 5639.97 | 0.913 | –40 | HeI | 4921.93 | 0.715 | –47 |
| SII | 5606.15 | 0.961 | –42 | SII | 4917.21 | 0.972 | –39 |
| | | | | Hβ | 4861.34 | 0.681 | –97 |

disappeared (2013 December 29–30), an ordinary P Cyg-type profile was visible (2014 February 07, 09–10, 13, 18) and again the process of formation of inverse P Cyg-type profile with very weak emission on the violet wing occurred (2014 August 27). On 2016 February 15, the Hα profile almost disappeared again.

The profiles of the Hα line, which were observed on 2014 February 07, 09, 10, 13 and 18, were normal P Cyg profiles. At these times, the RVs of absorption and emission components of the Hα lines varied from –179 to –88 km s$^{-1}$ and 7–17 km s$^{-1}$. This observational fact suggests that at this phase the atmosphere of the star was active and it indicates that there was matter flow to the upper layers of the stellar atmosphere and this star was surrounded by an envelope. This was an atmospheric expansion phase and the atmosphere of the star was non-stationary.

On 2013 December 25, and on 2014 August 27, we observed the inverse profile of the Hα. First, we determine the escape velocity of the star

$$\begin{aligned} V_{\rm esc} &= \sqrt{2G\frac{M_*}{R_*}} \\ &= \sqrt{2\times 6.67\times 10^{-11}\times\frac{24M_\odot}{52R_\odot}} \\ &= \sqrt{13.34\times 10^{-11}\times\frac{\rm Nm^2}{\rm kg^2}\times\frac{24\times 2\times 10^{30}\rm kg}{52\times 7\times 10^{8}\rm m}} \\ &\approx 420\,\rm km\,s^{-1}\,. \end{aligned}$$

As we can see from Table 5, on 2014 February 13 (Fig. 6) the RVs of Hα and Hβ lines, and the average velocity of the HeI lines are equal to –142 km s$^{-1}$, –97 km s$^{-1}$ and –47.5 km s$^{-1}$, respectively. It is apparent that only the RVs of the Hα and Hβ lines differ dramatically from the velocity of the mass center of the star. However, the

average velocities of most photospheric absorption lines are approximately the same as the velocity of the center of mass. From this observational fact, we can also draw conclusions about the dynamical stability of the deeper layers in which photospheric absorption lines are formed.

If we take into account the RV of the star ($V_{\rm r}' = -42.2$ km s$^{-1}$) and the RVs of layers where the indicated lines are formed, we determine the values of $-99.8$ km s$^{-1}$, –54.8 km s$^{-1}$ and –5.3 km s$^{-1}$, respectively. We can conclude that at that time there is an increasing rate of movement to the upper layers of the atmosphere, i.e. there is outflow of matter from the star, but the deep layers of the atmosphere of HD14134 are relatively stable.

Tables 3 and 4 also show that the absolute velocities of H$\alpha$ and H$\beta$ absorption lines are much lower than $V_{\rm esc}$. Therefore, the ejected matter (or outflow of matter) from the star cannot leave the gravitation of the supergiant star and this indicates that the return of the ejected matter to the star is observed. That is, formation of this inversion may be explained by the high-velocity motion of the stellar wind away from the observer. This also indicates that the inflow of matter to the star occurs in the effective layers in which the H$\alpha$ line is formed. We noted above that when the inverse H$\alpha$ profile is observed, the H$\beta$ line is redshifted.

As seen from Table 3, on these dates the absorption of the H$\alpha$ line is shifted toward the red and $V_{\rm r}({\rm abs}) = -13$ km s$^{-1}$ and $V_{\rm r}({\rm abs}) = -31$ km s$^{-1}$, respectively. At the same time, Figure 2(b) and Table 4 also show that the H$\beta$ line is also strongly redshifted and $V_{\rm r} = -30$ km s$^{-1}$ and $V_{\rm r} = -40$ km s$^{-1}$, respectively. This suggests that such synchronous changes may be due to the result of a strong stellar wind away from the observer. Note that inversion of the P Cyg profile in the spectra of this star is not always observed.

In this case, the star's atmosphere shows a contraction phase and is non-stationary.

Our observations indicated that the intensity of the H$\alpha$ line has sharply weakened on 2016 February 13, and on the other hand the H$\alpha$ line almost completely disappeared on 2013 December 29–30, and on 2016 February 15, in the spectra of the star HD14134 which probably is a manifestation of some recurrent processes in the star's atmosphere.

We suggest that when the matter composing the stellar wind moves away from the observer, the absorption component of the H$\alpha$ line is shifted toward the red region of the spectrum. Thus, the central frequencies (or wavelengths) of the absorption and emission components can coincide and compensate each other, which may lead to the disappearance of the H$\alpha$ profile (Kraus et al. 2015). That is, the disappearances of the H$\alpha$ line may be related to "swamping" of the absorption by emission.

Table 4 shows that at the time of the disappearance of the H$\alpha$ line or when its intensity sharply weakens, the H$\beta$ line is relatively redshifted and its RVs are –71 km s$^{-1}$, –74 km s$^{-1}$, –72 km s$^{-1}$ and –68 km s$^{-1}$. These observations may provide evidence for the fact that in the epochs when the H$\alpha$ line becomes faint, the layer of matter where H$\beta$ forms moves to the observer with lower velocity. However, significant changes in the RVs of other lines were not observed. H$\alpha$ and H$\beta$ lines are known to form in the upper layers of the stellar atmosphere, in the region where stellar wind is generated. The variability of this region of the atmosphere implies variability of the lines. These events may be a manifestation of a non-stationary atmosphere of the star or non-spherical stellar wind (Rosendhal 1973; Sobolev 1947, 1985).

Thus, disappearance of the H$\alpha$ line profile is not accompanied by significant changes in the spectral parameters of the other lines (except H$\beta$), so it is most likely due to the physical processes occurring in the upper atmosphere.

In this case, the atmosphere of the star is in the relative contraction phase (especially for the upper layers where H$\alpha$ forms) and is non-stationary.

It is known that variable stellar wind in supergiants is caused by pulsation (Cox 1983). If the disappearance of the H$\alpha$ line in the star HD14134 is associated with pulsation, they should occur periodically. However, the amount of obtained data and their inconsistency in terms of observation time do not make it possible to claim such far-reaching conclusions in this paper.

In addition, short-term and long-term changes in the RVs and spectral parameters of the H$\beta$ line have been revealed (Fig. 4). The RV of the H$\beta$ line has been changed by 67 km s$^{-1}$ (from –30 km s$^{-1}$ to –97 km s$^{-1}$) during $\sim 50 - 55$ d. If this can be considered as an amplitude of variation, then the value of pulsation period of the star can be considered approximately equal to $\sim 100 - 110$ d. Similar changes of HeI and CII lines with low amplitude ($\sim 18$ km s$^{-1}$ and $\sim 13$ km s$^{-1}$ correspondingly) during the same time have been observed (Fig. 5(a), (b)). The velocities of SiII lines show similar variability (Fig. 5(c)). For a more precise determination of the pulsation period of a star, systematic observations of this star are necessary.

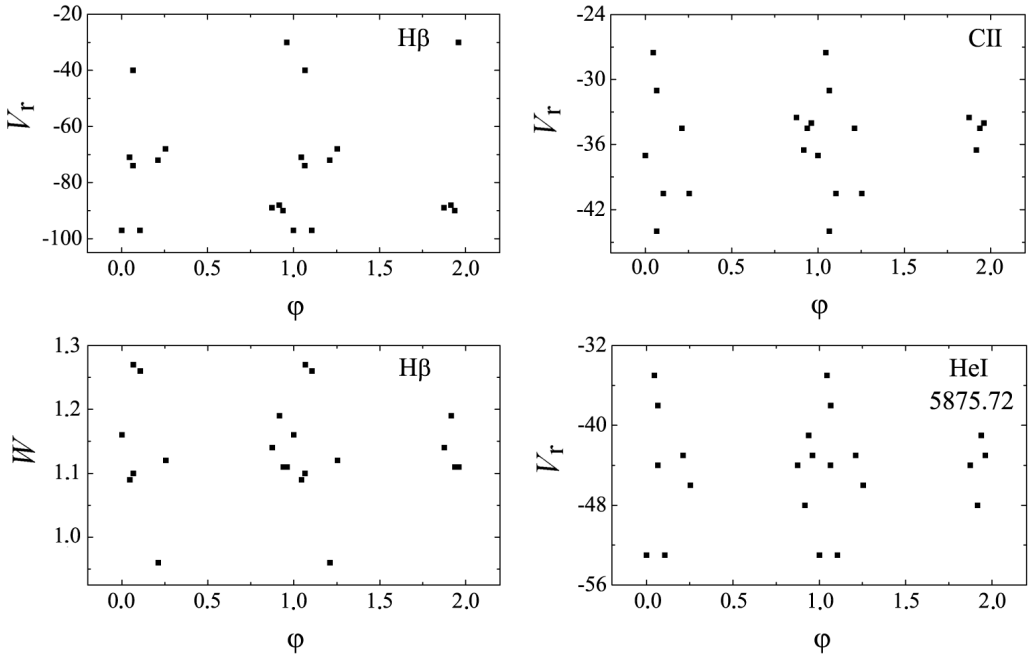


**Fig. 8** Variation with phase ($P_{\rm phot.}$=12.823 d) of the RVs, equivalent width in the H$\beta$ line, averaged CII ($\lambda$6578.05 Å, $\lambda$6582.88 Å) and HeI$\lambda$ 5875.72 Å. Zero phase is $T_0 = 2456702.19$.

On the other hand, it was revealed that significant variability happens in the CII and SiII line profiles. However, we did not observe strong changes in the structure of profiles of HeI $\lambda$ 5875.72 Å, or in other photospheric lines. Note that the line HeI $\lambda$ 5875.72 Å is not really photospheric and it frequently shows a P Cyg type profile in most supergiants. Our measurements of this line show strong RV variability and due to the significant line strength it is difficult to detect structural changes in the line profile. Still, the line profile is expected to be slightly variable. In addition, we confess that we cannot detect variations in other photospheric lines because these lines are weak, and also the detected variable lines are the strongest absorption lines in the spectra and are partially formed in the wind.

Why are photospheric lines variable?

The period analysis by Lucy (1976) of RV curves of $\alpha$ Cyg revealed the simultaneous excitation of multiple pulsational modes including radial modes and low-order non-radial g modes.

Kaufer et al. (1997) obtained time series of spectra with high S/N and high resolution in wavelength and time of BA-type supergiants. In that work they inspected the time variations of numerous photospheric line profiles in the optical spectrum. They did not find any depth dependence of the velocity fields in the metallic lines of these supergiants in their sample. The analysis of the line-profile variations (LPV) of the photospheric line spectrum revealed prograde traveling features in the dynamical spectra. The traveling times of these features are in contradiction to the possible rotation periods of these extended, slowly rotating objects. Therefore, they identified these features with non-radial pulsation modes.

Hence, we suggest that all variations can be reasonably explained by stellar wind properties (Kudritzki et al. 1999; Morel et al. 2004; Kraus et al. 2015) and/or pulsation mechanisms (Kaufer et al. 1997; Lucy 1976).

Figures 8 and 9 present variations with phase ($P_{\rm phot.} = 12.823$ d and $P_{\rm phot.} = 1.625$ d) of RVs, equivalent width in the H$\beta$, averaged CII ($\lambda$6578.05 Å, $\lambda$6582.88 Å) and HeI$\lambda$ 5875.72 Å. We also attempt to correlate our spectroscopic data with the photometric periods of 12.823 and 1.625 d found by Morel et al. (2004) and Lefèvre et al. (2009), but no correlation was found.

For detailed investigation of these events, additional systematic observations of these stars with high resolution are planned at Shamakhy Astrophysical Observatory in the near future.

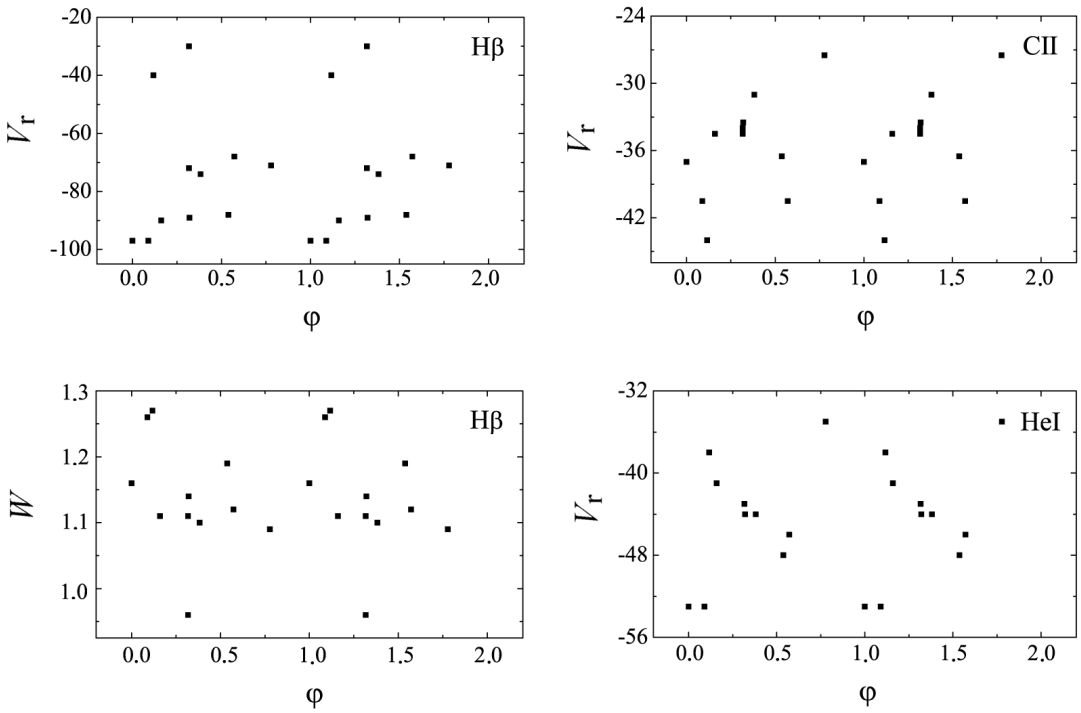


**Fig. 9** Variation with phase ($P_{\rm phot.} = 1.625$ d) of the RVs, equivalent width in the H$\beta$, averaged CII ($\lambda$6578.05 Å, $\lambda$6582.88 Å) and HeI$\lambda$5875.72 Å. Zero phase is $T_0 = 2456702.19$.

## 4 CONCLUSIONS

The disappearance of the H$\alpha$ line in the spectra of supergiant star HD14134 was demonstrated for the first time. This behavior is real and recurrent. We suggest that the disappearance of the H$\alpha$ line may be related to swamping of the absorption by emission (Kraus et al. 2015). These events may be a manifestation of a non-stationary atmosphere of the star or non-spherical stellar wind. When the H$\alpha$ line disappears or becomes faint, the H$\beta$ line is relatively redshifted.

An inversion of the P-Cyg-type profile of the H$\alpha$ line is observed on two days in the spectra of the star HD14134. Formation of this inversion may be explained by the high-velocity motion of the stellar wind matter away from the observer. At these times, the H$\beta$ line is strongly redshifted.

The repetition of normal and inverse P Cyg profiles is mainly accompanied by expansion and contraction of the atmosphere of the star HD14134 (Wolf & Stahl 1990). However, disappearance of the H$\alpha$ line is accompanied by relative contraction (especially for the upper layers where H$\alpha$ forms) of the star's atmosphere.

When the H$\alpha$ line disappeared or an inversion of the P-Cyg-type profile is observed in the spectra, no synchronous variabilities were observed in other spectral lines formed in deeper layers of the stellar atmosphere, including HeI, CII and SiII lines.

We found that line profile variability was already evident on timescales as short as half an hour, probably due to the presence of pulsations. As of today, such monitoring has been carried out for only very few massive stars (Hubrig et al. 2014; Kholtygin et al. 2017). The detected short-time variability should be studied in more detail by future spectroscopic and photometric monitoring of this supergiant.

In addition, we revealed significant variabilities in the structures and RVs of CII and SiII lines. We suggest that the LPV of the photospheric lines are basically caused by non-radial pulsation (Kaufer et al. 1997). However, we did not observe strong changes in the structure of profiles of HeI $\lambda$ 5875.72 Å or in other photospheric lines. Because our measurements of the HeI line show strong RV variability and due to the significant line strength, it is difficult to detect structural changes in the line profile. Still, the line profile is expected to be slightly

variable. On the other hand, we cannot detect variations in other photospheric lines because these lines are weak in the spectra.

Hence, we suggest that all variations can probably be explained by stellar wind properties (Kudritzki et al. 1999; Morel et al. 2004; Kraus et al. 2015) and/or pulsation mechanisms (Kaufer et al. 1997; Lucy 1976).

We found no correlation of the spectroscopic variability with the photometric periods of 12.823 and 1.625 d for the star HD14134 found by Morel et al. (2004) and Lefèvre et al. (2009).

**Acknowledgements** I am grateful to the reviewer and Prof. N.Z. Ismailov for their attentions to this study. This work was supported by the scientific program for priority fields of research of the National Academy of Sciences of Azerbaijan.

## References

Barlow, M. J., & Cohen, M. 1977, ApJ, 213, 737

Chentsov, E. L., et al. 2003, A&A, 397, 1035

Cox, J. P. 1983, Theory of Stellar Pulsations. (Translated from the English Edition. Mir, Moskva. 326 (1983). in Russian)

Crowther, P. A., Lennon, D. J., & Walborn, N. R. 2006, A&A, 446, 279

Galazutdinov G. A., 1992, Preprint SAO RAN, Spets. Astrofiz. Nizhnii Arkhyz, KChR, 92, *https://www.sao.ru/hq/coude/galazut.htm*

Galazutdinov, G., Strobel, A., Musaev, F. A., Bondar, A., & Krełowski, J. 2015, PASP, 127, 126

Hubrig, S., Schöller, M., & Kholtygin, A. F. 2014, MNRAS, 440, 1779

Hutchings, J. B. 1970, MNRAS, 147, 161

Hutchings, J. B. 1976, Publications of the Dominion Astrophysical Observatory Victoria, 14, 355

Kaufer, A., Stahl, O., Wolf, B., et al. 1997, A&A, 320, 273

Kholtygin, A. F., Hubrig, S., Dushin, V. V., et al. 2017, arXiv:1701.00733

Kontizas, E., & Kontizas, M. 1981, A&AS, 45, 121

Kraus, M., et al. 2015, A&A, 581, A75, 1

Kudritzki, R. P., Puls, J., Lennon, D. J., et al. 1999, A&A, 350, 970

Lefèvre, L., Marchenko, S. V., Moffat, A. F. J., & Acker, A. 2009, A&A, 507, 1141

Lucy, L. B. 1976, ApJ, 206, 499

Mikailov Kh. M., Khalilov, V. M., & Alekberov, I. A, 2005, Tsirk. Shamakhy Astrophys. Observ., 109, 21

Morel, T., Marchenko, S. V., Pati, A. K., et al. 2004, MNRAS, 351, 552

Rosendhal, J. D. 1973, ApJ, 186, 909

Santolaya-Rey, A. E., Puls, J., & Herrero, A. 1997, A&A, 323, 488

Sobolev, V. 1947, Moving Envelopes of Stars (in Russian) (Leningrad State University)

Sobolev, V. V. 1985, Course in Theoretical Astrophysics (3rd revised and enlarged edition, in Russian), 504 (Moscow: Izdatel'stvo Nauka)

Gontcharov, G. A. 2006, Astronomy Letters, 32, 759

Tarafdar, S. P. 1988, ApJ, 331, 932

Wilson, I. R. G., & Dopita, M. A. 1985, A&A, 149, 295

Wolf, B., & Stahl, O. 1990, A&A, 235, 340